Forecasting Large Hail and Lightning using Additive Logistic Regression Models and the ECMWF Reforecasts

Francesco Battaglioli[1,2], Pieter Groenemeijer[1,3], Ivan Tsonevsky[4], Tomàš Púčik[3]

[1]European Severe Storms Laboratory e.V. (ESSL), Wessling, 82234, Germany
[2]Institut für Meteorologie, Freie Universität Berlin, Berlin, 12165, Germany
[3]European Severe Storms Laboratory (ESSL) – Science and Training, Wiener Neustadt, 2700, Austria
[3]European Centre for Medium Range Weather Forecasts (ECMWF), Reading, RG2 9AX, United Kingdom

Correspondence to: Francesco Battaglioli (francesco.battaglioli@essl.org)

Abstract. Additive Logistic Regression models for lightning (AR_{lig}) and large hail (AR_{hail}) were developed using convective parameters from the ERA5 reanalysis, hail reports from the European Severe Weather Database (ESWD), and lightning observations from the Met Office Arrival Time Difference network (ATDnet). The models yield the probability of lightning and large hail in a given timeframe over a particular grid point. To explore the value of this approach to medium-range forecasting, the models were applied to the European Centre for Medium Range Weather Forecasts (ECMWF) reforecasts to reconstruct probabilistic lightning and large hail forecasts for 11 ensemble members, from 2008 to 2019 and for lead times up to 228 hours. The lightning and large hail models were based on different predictor parameters: most unstable convective available potential energy (CAPE), 925 – 500 hPa bulk shear, mixed layer mixing ratio, wet bulb zero height (for large hail); most unstable lifted index, mean relative humidity between 850 and 500 hPa, one hourly accumulated convective precipitation and specific humidity at 925 hPa (for lightning). First, we compared the lightning and hail ensemble forecasts for different lead times with observed lightning and hail focusing on a recent hail outbreak. Secondly, we evaluated the model's predictive skill as a function of forecast lead time using the Area under the ROC Curve (AUC) as a validation score. This analysis showed that AR_{hail} has a very high predictive skill (AUC > 0.95) for a lead time up to 60 hours. AR_{hail} retains a high predictive skill even for extended forecasts (AUC = 0.86 at 180 hours lead time). Although AR_{lig} exhibits a lower predictive skill compared AR_{hail}, lightning forecasts are also skillful both in the short term (AUC = 0.92 at 60 hours) and in the medium range (AUC = 0.82 at 180 hours). Finally, we compared the performance of our four-dimensional hail model with that of composite parameters such as the Significant Hail Parameter (SHP) or the product of CAPE and the 925 – 500 hPa bulk shear (CAPESHEAR). Results show that AR_{hail} outperforms CAPESHEAR at all lead times and SHP at short to medium lead times. These findings suggests that the combination of Additive Logistic Regression models and ECMWF ensemble forecasts can create highly skilful medium-range hail and lightning forecasts for Europe.

1 Introduction

Lightning and large hail are responsible every year of large societal and economic impacts in Europe. While hail is mostly responsible for high economic losses with single events causing more than 1 billion US dollars (Púčik et al. 2019), lightning is responsible for hundreds of injuries and an average of 64 fatalities per year only in Europe (Kühne et al. 2023). Such extensive economic and societal impacts have sparked research on different aspects of these events ranging from the development of climatologies (hail: Cintineo et al. 2012; Cecil and Blankenship 2012; Bang and Cecil 2019; Púčik et al. 2019; Taszarek et al. 2020a; Fluck et al. 2021; Murillo et al. 2021, lightning: Feudale et al. 2013; Wapler 2013; Taszarek et al. 2019; Enno et al. 2020), to nowcasting (hail: Ryzhkov et al. 2013; Ortega et al. 2016; Nisi et al. 2020; Schmidt 2020, lightning: Mostajabi et al. 2019; Cintineo et al. 2022; Leinonen et al. 2022) and forecasting (hail: Jewell and Brimelow 2009; Adams-Selin and Ziegler 2016; Czernecki et al. 2019; Allen et al. 2020, lightning: McCaul et al. 2009; Zepka et al. 2014; Dafis et al. 2018; Geng et al. 2021). Lightning can be forecasted based on the pre-convective environment using the ingredient-based methodology (Johns and Doswell 1992) of deep-moist convection for which convective storms require three ingredients to form: conditional instability, moisture and lift. Although all convective storms require these three ingredients, not all of them produce lightning. Van Den Broeke et al. (2004) found that sufficient instability must exist in the lower mixed phase region of the cloud for lightning to occur. Their findings have been used to create a physical-based parameter for lightning prediction at the Storm Prediction Center (Bright et al. 2004). Westermayer et al. (2017) have found that the relative frequency of lightning increases as CAPE grows between 0 and 200 J/kg, levelling off after that. The frequency only increases further once the mid-tropospheric relative humidity increases and/or CIN decreases. Another approach to lightning forecasting is using explicit simulations a thunderstorm updraft and its microphysics. This is the case for the Lightning Potential Index (LPI) developed by Yair et al. (2010) and applied in a number of convection-allowing models (Lagasio et al. 2017, Brisson et al. 2021, Uhlirova et al. 2022. For global, lower resolution models, a combination of pre-convective environment and cloud properties has been used to parameterize lightning (Lopez, 2016). Hail forecasting techniques have been widely explored in the United States both with the development of hail models based on the explicit simulation of hail growth mechanisms in a thunderstorm e.g., HAILCAST (Brimelow 2002; Brimelow and Jewell 2009; Adams-Selin and Ziegler 2016) but also with the use of convection allowing models (Gallo et al. 2016, 2018) and convection allowing ensembles (Loken et al. 2020). In Europe, hail research has mostly concentrated on (semi-) automatic nowcasting techniques using radar data (Martius et al. 2015). Although successful medium-range hail forecasts can mitigate the impacts of hail and have been shown to be skilful in the United States (Lepore et al. 2017, 2018), little attention has been given to the development of specific products for medium-range hail forecasting in Europe. At such lead times, convection allowing models are not available, but an ingredients-based approach (Doswell et al. 1996) can be used, whereby forecasters look for the simultaneous presence of prerequisites needed to sustain hailstorms, such as instability, moisture, lift, and a minimum amount of wind shear. Composite parameters such as the Large Hail Parameter (LHP; Johnson and Sugden 2014), the Supercell Composite Parameter (SCP; Thompson et al. 2004) and the Significant Hail Parameter (SHP; http://www.spc.noaa.gov/exper/mesoanalysis/help/help_sigh.html) can help by combining

several ingredients into one number describing whether the environmental conditions are supportive for large hail and can be used for medium-range forecasting. SHP calculated from the Global Ensemble Forecast System (GEFS) yielded skilful probabilistic hail forecasts up to 12 days in advance in the United States (Gensini and Tippett, 2019). Although composite parameters such as SHP perform well across the United States, climatologies based on them perform worse across regions where the parameter has not been specifically developed (e.g., Europe as found by Taszarek et al. 2020b). Battaglioli et al. (2023) showed that the Additive Logistic Regression Models (AR-CHaMo) for large hail occurrence have a better predictive skill than SHP and can result in a more realistic climatological distribution of hail occurrence across Europe. Building upon these findings, in this study we leverage an ensemble approach in conjunction with the lightning and hail models from Battaglioli et al. (2023) to yield probabilistic lightning and hail forecasts with the ultimate goal of improving medium-range forecasting of these hazards in Europe.

2 Data

2.1 AR-CHaMo lightning and hail models

The AR-CHaMo models were developed by Rädler et al. (2018) and improved by Battaglioli et al. (2023). The models were trained using lightning observations from the Arrival Time Difference Network (ATDNet, Anderson and Klugmann 2014; Enno et al. 2020), hail reports from the European Severe Weather Database (ESWD; Dotzek et al. 2009; Groenemeijer et al. 2017) and convective parameters from the ERA5 reanalysis (Hersbach et al. 2020). The model training area for large hail was limited to Central Europe (Figure 1b) where the reporting of severe weather in the ESWD is the highest (Groenemeijer and Kühne 2014; Taszarek et al. 2020a). This was done to limit sampling of situations in our training dataset that could have affected the model development, namely when hail occurred but was not reported to the ESWD. The lightning model training region covered a much larger area (Figure 1a) since the detection efficiency of ATDnet is homogenous across the European domain. Lightning and hail reports were gridded on a 0.25° x 0.25° grid box, the same horizontal resolution of the ERA5 reanalysis. In addition, the time of reports was rounded down to the nearest full hour. This allowed to best sample the pre-convective environment associated with each lightning observation or hail report as done by Rädler et al. (2018) and Taszarek et al. (2021b). The AR-CHaMo models use logistic regression to assign a probability of hazard occurrence as a function of reanalysis-derived predictor parameters. AR-CHaMo separately predicts the probability of thunderstorm formation and the probability of large hail (≥ 2 cm) given that a thunderstorm formed. The probability of large hail ($P_{hail>2cm}$) is a product of these two components as shown in Eq. (1):

$$P_{hail>2cm} = P_{lightning} \cdot P_{hail>2cm|lightning} \qquad (1)$$

Different predictor parameters from the ERA5 reanalysis were selected for the lightning and the hail model following a model selection procedure based on an ingredients-based approach (Johns and Doswell 1992), the Deviance Explained (Wood 2006) and the Bayesian Information Criterion (BIC, Schwarz 1978) score. Out of 172 available parameters from the ERA5 reanalysis,

the model selection procedure with Deviance Explained (the higher, the better) and BIC (the lower, the better) yielded a 5-dimensional lightning model and a 4-dimensional conditional hail ≥ 2 cm model. More details on the model selection procedure can be found in Battaglioli et al. (2023) while the final model predictors for the lightning and the conditional hail models are listed in Table 1.

2.2 ECMWF forecast data

Forecast data across Europe were obtained from the European Centre for Medium Range Weather Forecasts (ECMWF) reforecasts (Vitart, 2014) for the period 2008-2019. ECMWF reforecasts used in this study consist of 10 perturbed ensemble members and 1 control forecast run every Monday and Thursday. These reforecasts, unlike reanalysis, always use the operational version of ECMWF's Integrated Forecasting System (IFS), covering two IFS cycles: 46r1 until the 30th of June 2020 and 47r1 afterwards. Such change in IFS cycle is however not expected to have caused discontinuities in convective parameters calculation (e.g., in CAPE) since the convection scheme was not modified from 46r1 to 47r1. Reforecast data were extracted at a spatial resolution of 0.2° x 0.2° and 6-hourly temporal resolution. The forecast parameters downloaded from reforecasts were temperature, specific humidity, u and v wind components at the 1000, 850, 700 and 500 hPa pressure levels. They were used to compute convection related parameters such as mixing ratio, mid-level relative humidity, 925 to 500 hPa bulk shear (deep layer shear). Composite parameters, such as Convective Available Potential Energy (CAPE)-shear (a product of $\sqrt{CAPE}$ and deep layer shear) and SHP were also calculated while CAPE for the most-unstable parcel (MUCAPE) and convective precipitation were obtained directly from the IFS.

2.3 Lightning observations and hail reports

Lightning data from ATDnet were used to verify lightning forecasts from AR-CHaMo. This network can detect lightning flashes even at large distances from a sensor and allows verification of the lightning forecasts across a broad region covering most of Europe. Data was obtained for the period 2008–2019, gridded on a 0.2° x 0.2° box to allow for direct comparison to ECMWF reforecasts, and organized as a binary field indicating whether a lightning case occurred (1 = yes, 0 = no). A lightning case was defined as a three-hour period with at least 2 lightning strikes per grid box. Following Rädler et al. (2018), single detections were ignored as they might be isolated measurement errors rather than lightning. Hail reports were obtained from the ESWD and used to verify the hail forecasts. As per Rädler et al. (2018), reports with an excessive time uncertainty (> 1 hour) were discarded from the verification dataset. In total, 10872890 lightning observations and 5493 reports of large hail were considered within the verification dataset.

3 Model development and adaptation

The models for lightning and large hail developed in Battaglioli et al. (2023) were based on the predictors from the ERA5 reanalysis listed in Table 1. Owing to the limited vertical resolution of the ECMWF reforecast data, some of the original AR-

CHaMo predictors (e.g., MU500_CAPE-10°) could not be calculated using the ECMWF reforecasts. For this reason, the models were adapted using predictors as close as possible to their original versions (e.g., MU_CAPE was chosen instead of MU500_CAPE-10°). The models were then trained again using the adapted predictors (shown in Table 2) using ERA5 reanalysis, lightning and hail observations. The models were not retrained using the ECMWF reforecasts owing to the nature of the dataset: reforecasts are initialised only two times a week and the representation of the environmental conditions in proximity of a report is dependent on the forecast lead time (the closer to the initialization time, the better). For instance, if two hail reports occurred on Tuesday at 12:00 UTC and on Wednesday at 18:00 UTC it would not be possible to qualitatively compare the environmental conditions at these two time steps for a forecast initialized on Tuesday at 00 UTC meaning that the environmental conditions associated with the Wednesday at 18:00 UTC report would be subject to larger uncertainty due to the larger lead time. The models based on ERA5 assign a probability of hazard occurrence as a function of the reanalysis-derived predictor parameters listed in Table 2 to any location in a 0.25° x 0.25° grid and 1 hourly intervals. Given the different spatial (ERA5: 0.25° x 0.25°, ECMWF reforecast: 0.20° x 0.20°) and temporal (1 hour, 6 hours) resolution between ERA5 and ECMWF reforecasts, the probabilities had to be readapted. To account for the different spatial resolution of ECMWF reforecasts, the ERA5 $P_{hazard(ERA5)}$ probabilities were adapted following Eq. (2):

$$P_{hazard(ECMWF)} = 1 - (1 - P_{hazard_{(ERA5)}})^{A_{ECMWF}/A_{ERA5}} \qquad (2)$$

Where:

A_{ECMWF} is the Area of an ECMWF reforecast grid box (km^2)

A_{ERA5} is the Area of an ERA5 grid box (km^2)

$P_{hazard(ECMWF)}$ is the adapted probability using an ECMWF reforecast grid (%)

Given that ECMWF reforecasts are available every 6 hours, lightning and large hail probabilities could be calculated only at 4 different hourly time steps during the day (00:00 – 01:00, 06:00 – 07:00, 12:00 – 13:00, 18:00 – 19:00 UTC). Using only 4 hourly time steps would significantly limit the amount of large hail reports to work with for verification. Therefore, probabilities were upscaled to three-hour intervals (00:00 – 03:00, 06:00 – 09:00, 12:00 – 15:00, 18:00 – 21:00 UTC) following Eq. (3), based on the assumption that each hour probability is independent of that in another hour:

$$P_{hazard(3\ hourly)} = 1 - (1 - P_{hazard_{(1\ hourly)}})^3 \qquad (3)$$

With these adaptations, we applied the AR-CHaMo based on ERA5 to ECMWF reforecasts yielding 3 hourly ensemble lightning and hail probabilistic forecasts at 0.2° x 0.2° spatial resolution for the period 2008-2019 and for the whole of Europe.

4 Application of hail and lightning models to a case study: 15th of June 2019

4.1 Ensemble Forecasts

We first tested the AR-CHaMo-based lightning and hail forecasts on a case study. On the 15th of June 2019, severe storms with large hail occurred in eastern Germany, western-Poland and Czechia. More than 20 hail reports were submitted for the period of 12:00 –15:00 UTC with several hail reports exceeding 5 cm in diameter. A second region of interest on the day was south-eastern France where very large hail was also reported (8 cm near Grenoble). We evaluated the performance of the ensemble forecasts depending on the lead time by considering ECMWF reforecasts initialized at three different lead times (T-12h, T-108h and T-180h) ahead of the event. To allow for a comparison with hail forecast products from the U.S. Storm Prediction Centre (SPC), probabilities were upscaled using an adapted version of Equation 2 to yield a probability of hail ≥ 2 cm occurrence in a radius of 25 miles of a point, approximately 40 km. For hail forecasts for the 15th of June 2019 at 12:00 UTC, initialized at 00:00 UTC on the same day, a strong agreement between all ensemble members was present in identifying the Germany-Poland-Czechia region and south-eastern France as the areas with highest hail potential ($P_{hail>2cm} > 30$ %) (Figure 2). To compare the AR-CHaMo forecast with that of existing composite parameters, we produced probabilistic hail forecasts for the same timestep and initialization time based on two 1-dimensional logistic models trained using SHP (Figure 3) and CAPESHEAR (Figure 4). The SHP model is in agreement regarding the Germany-Poland-Czechia and south-eastern France regions, but compared to AR-CHaMo, yields high hail probabilities also across regions where no hail was reported e.g., the Balkans and Eastern Europe. The CAPESHEAR model, on the other hand, identifies well the south-eastern France region but places the highest probability of hail across northern Germany and northern Poland away from the highest density of hail reports to the south. Similarly to the hail forecasts, there was a strong agreement in the lightning forecast among the ensemble members at 12 hours lead time (Figure 5). A high probability of lightning ($P_{lightning} > 80$%) was present across the German-Polish border and south-eastern France. Between 12:00 and 15:00 UTC, widespread lightning activity occurred across a broad region extending from Northern Germany and Denmark all the way south to southern Austria, verifying the lightning forecast in these areas. In addition to these regions, high lightning probabilities were found along a corridor extending from Ukraine into Russia. Widespread lightning activity was also observed here. An underestimation of the lightning activity was present across western Türkiye, where thunderstorms occurred despite low CAPE (< 100 $J\ kg^{-1}$; see sounding in Appendix A).

4.2 Physical interpretation of model forecasts

Forecast soundings and hodographs can show how individual parameters influenced the probability of lightning or hail simulated by AR-CHaMo. Two regions, central Ukraine and central Italy, showed respectively high and low probabilities of lightning (Figure 6). While moderate buoyancy (CAPE > 1000 Jkg^{-1}) was present in both regions, the main difference in the two profiles was the mid-level relative humidity, significantly lower in the Italian sounding. Here a deep, dry layer in the mid-troposphere could have resulted in dry air entrainment of updrafts that inhibited convective initiation (Rädler et al. 2018, Poręba et al. 2022). The comparison between hail and lightning forecasts highlights the model's ability to distinguish between

areas with lightning potential and with hail potential. In a region extending from Romania into Ukraine and Russia, low probabilities of large hail ($P_{hail>2cm}$ < 10 %) were found (Figure 2) alongside high lightning probabilities ($P_{lightning}$ > 70 %, Figure 5). On the other hand, across eastern Germany the probabilities of lightning ($P_{lightning}$ > 70 %) and hail ($P_{hail>2cm}$ > 25 %) were both relatively high. While high CAPE was present both across Ukraine and eastern Germany, the deep-layer shear was much stronger over Germany. Stronger shear is associated with a higher likelihood of large hail, because it promotes storm organisation (Thompson et al. 2012; Johnson and Sugden 2014; Púčik et al. 2015; Taszarek et al. 2020b; Kumjian et al. 2021). This was well reflected by AR-CHaMo that showed a higher hail probability across eastern Germany in correspondence of the strongest shear.

4.3 Forecast dependence on lead time

We next investigated how lead time affects forecast performance by comparing the forecast for the 15th of June 2019 at 12:00 UTC initialised on the 11th of June 2019 at 00:00 UTC (T-108 h, Figure 8) with the T-12h forecast (Figure 2). Despite the increased lead time, the ensemble members were still in good agreement regarding the location of the highest hail probabilities across the German-Polish-Czech area even 4 days in advance. The largest difference compared to the T-12-hour forecast was found across south-eastern France where most members showed no probability of large hail occurrence.

The reason for the large spread in the hail probabilities was a large spread in the predicted CAPE (Figure 10), which was much lower for shorter lead times (Figure 9). While the T-12-hour forecast highlights a localised spot of high CAPE across south-eastern France, this region of enhanced buoyancy was not represented by most members in the T-108-hour forecast. Forecasts of deep-layer shear (not shown) for the two lead times did not show differences that might impact the forecast across south-eastern France. As the lead time and spread among the forecast members increased, the mean probabilities decreased (Figure 11). A similar dependence on the lead time was observed for the 1-dimensional logistic models based on SHP and CAPESHEAR (Appendix B). Despite the increased spread compared to the T-12-hour forecast, the T-108-hour hail forecast had a good predictive skill across the German-Polish-Czech area with a widespread 10 – 15 % probability of occurrence, that could be clearly distinguished from surrounding areas with very low probabilities. The T-108-hour lightning forecast (Appendix C) was also in good agreement with the T-12-hour forecast, although lower confidence was found across Eastern Europe where uncertainty regarding the location of the initiation boundary existed. The spread increased further in the T-180-hour forecast for both hail and lightning (Figure 11). For this case study we showed that the logistic model applied to the ECMWF reforecasts provided a skilful forecast at least up to 108 hours in advance for both hail and lightning. The loss of predictive skill from 12 to 108 hours for the hail model was mostly caused by an increasing uncertainty in the CAPE forecast with increasing lead time.

5 Model Evaluation

In order to provide an evaluation of the model's skill not tied to a single case study, the ensemble mean of the forecasted probabilities of AR-CHaMo on the individual ensemble members were systematically verified at four different times during

the day (00:00 UTC, 06:00 UTC, 12:00 UTC, 18:00 UTC) against lightning observations from ATDnet in the one hour following the forecast time (00:00 – 01:00 UTC, 06:00 – 07:00 UTC, 12:00 – 13:00 UTC, 18:00 – 19:00 UTC) and hail reports from the ESWD in the three hours following the forecast time (00:00 – 03:00 UTC, 06:00 – 09:00 UTC, 12:00 – 15:00 UTC, 18:00 – 21:00 UTC). While for lightning the full European domain was used to verify lightning forecasts owing to the homogenous detection efficiency of ATDnet across the domain, hail forecasts were only verified against ESWD hail reports in Central Europe (Figure 1b). This reduced area was chosen because of a lack of reports from some regions, such as south-eastern Europe (Rädler et al. 2018). We used the Receiver Operating Characteristic (ROC) curves for lead times from 12 to 228 hours (at 24-hour time steps) to investigate changes in forecast skill of the lightning and hail models, similarly to Tsonevsky et al. (2018). The Area Under the ROC Curve (AUC, Wilks 1995) measures the ability of the hail (lightning) model to discriminate between hail (lightning) and non-hail (non-lightning) situations. AUC values can range from 0 to 1: a model that has an AUC of 0.5 has the same skill of random guessing, the closer the AUC is to 1 the better the model can classify observations into classes – 0.8 to 0.9 is considered excellent, more than 0.9 is considered outstanding (Hosmer et al. 2013). The AUC scores for the hail model were higher than the lightning model ones at all lead times (Figure 12). The hail model exhibited a very high predictive skill: AUC > 0.95 for lead times up to 60 hours. Although the predictive skill decreased with increasing lead time, a high AUC was still found for lead times up to 108 hours. A relatively strong discontinuity in predictive skill was found between 108 (0.92) and 132 hours (0.87) and after 180 hours. The lightning model exhibited an almost linear decrease of predictive skill with increasing lead time. The performance of AR_{hail} was compared with that of 1-dimensional logistic models trained using CAPESHEAR and SHP as predictors and the same training dataset as for AR_{hail}. In Figure 13 we display the AUC scores for AR_{hail} and for the models based on the two composite parameters as a function of the forecast lead time. To quantify the uncertainty in the AUC for the different models we performed a 1000-member block bootstrap procedure as done by Hamill et al. (2018) that allowed us to determine the corresponding 95% confidence intervals. Comparing the AUC scores of the probabilistic forecasts based on the 1-dimensional CAPE-shear model and those of AR_{hail}, we concluded that AR_{hail} outperformed CAPESHEAR at all lead times. Compared to SHP, AR_{hail} had a higher performance at short-to-medium range (up to 60-84 hours) while with increasing lead time the two metrics became comparable in terms of predictive skill. It is hypothesised that the increase in the uncertainty of the atmospheric predictors was responsible for the loss of skill with increasing lead time, as shown for CAPE in Section 4.3.

6 Conclusion

We applied AR-CHaMo for lightning and large hail to the ECMWF reforecasts to develop probabilistic ensemble forecasts for the period 2008-2019 across Europe. In a case study of the 15th of June 2019, the models provided skilful guidance both for large hail and lightning up to 108 hours. The loss of skill with increasing lead time was mostly due to increased spread in CAPE. The predictive skill of the hail model was quantified in terms of AUC scores as a function of lead time: at short to medium ranges hail forecasts are highly skilful (≥ 0.95 up to 60 hours) and outperform all composite indices. The skill decreases progressively, most rapidly after 108 hours in lead time. Some limitations of this study must be considered with the

interpretation of these results. First, the limited vertical resolution of the ECMWF reforecasts did not allow the exact models developed using ERA5 to be applied, since some of the original predictors could not be calculated due to the limited reforecast

440   data availability. The atmospheric variables selected as predictors in place of the ERA5 ones can only approximate the original predictors and are likely not fully representative of the models developed using ERA5. It is important to note that although the original, more skilful, predictors from ERA5 could not be calculated, the adapted versions still managed to outperform state-of-the-art predictors such as SHP (at short lead times) and CAPESHEAR (at all lead times). Another limitation is that forecasts were only available four times a day, at 6 hours intervals, due to the limited temporal resolution of ECMWF re-forecasts.

445   Given the convective nature of these events it is likely that some hail events for verification were missed in the 6-hours intervals between each forecast. To reduce this, forecasts were verified against hail reports in the three hours following the forecast time.

Apart from these limitations, the developed models represent an improvement compared to state-of-the-art composite parameters in Europe. Future work will involve the application of the full ERA5 models to Numerical Weather Prediction

450   (NWP) to develop hail forecasts operationally and on a pan-European scale. A significant improvement in predictive skill is expected with the use of the most skilful predictors calculated form the ERA5 reanalysis. An extension of this approach to different convective hazards such as severe convective wind gusts and tornadoes can also be foreseen.

455

460

465

470

475

Model	Lightning	Hail ≥ 2 cm
Predictors	MU_LI (K) RH_500–850hPa (%) 1h Acc. Conv. Precip. (Kg m^{-2}) MU MIXR (g kg^{-1}) Land-sea Mask	MU500_CAPE-10° (J kg^{-1}) EFF_MU_BS (m s^{-1}) MU_MIXR (g kg^{-1}) 0° height (m)

Table 1: Selected predictor parameters for the original AR-CHaMo models. Acronyms are explained in Appendix D.

Model	Lightning	Hail ≥ 2 cm
Predictors	MU_LI (K) RH_500–850hPa (%) 1h Acc. Conv. Precip. (Kg m^{-2}) Specific humidity at 925 hPa (g kg^{-1}) *	MU_CAPE (J kg^{-1}) * Deep Layer Shear (m s^{-1}) * Specific humidity at 925 hPa (g kg^{-1}) * Wet Bulb Zero Height (m)

480

Table 2: Chosen predictor parameters for the regression models to be applied to the ECMWF reforecasts. Predictors highlighted with a star are the ones that have been changed compared to the original ERA5 ones listed in Table 1.

485
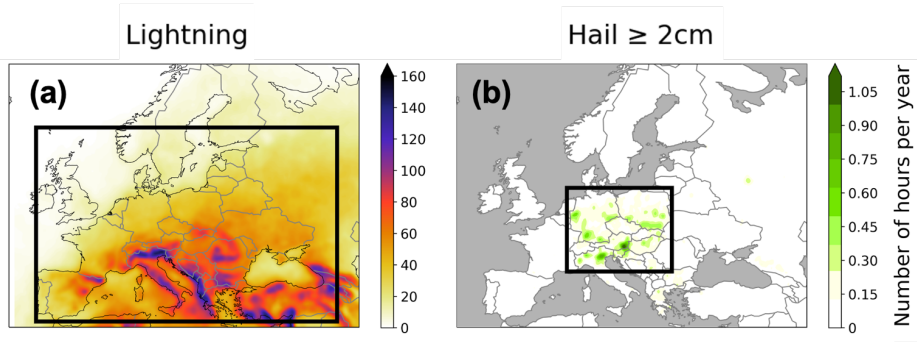
Figure 1: Annual mean distribution of lightning (a) and hail ≥ 2 cm (b) for the period 2008-2019. The black squares in (a) and (b) indicate the training regions for lightning (34.5° – 63.5°N, -9.0° – 46.0°W) and hail ≥ 2 cm (45.0° – 54.0°N, 5.0° – 22.0°W). Adapted from Battaglioli et al. (2023).
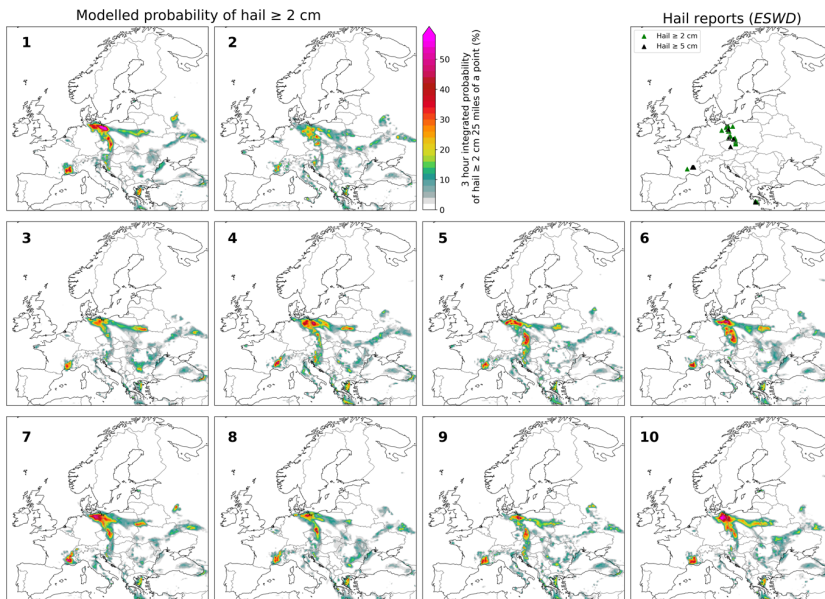
495 **Figure 2: Probabilistic forecast of hail ≥ 2 cm occurrence on the 15th of June 2019 at 12:00 UTC (initialized on the 15th of June 2019 at 00:00 UTC) for the individual ensemble members. Hail reports between 12:00 UTC and 15:00 UTC are shown as triangles (green for hail ≥ 2 cm but ≤ 5 cm, black for hail ≥ 5 cm) in the right-top panel.**
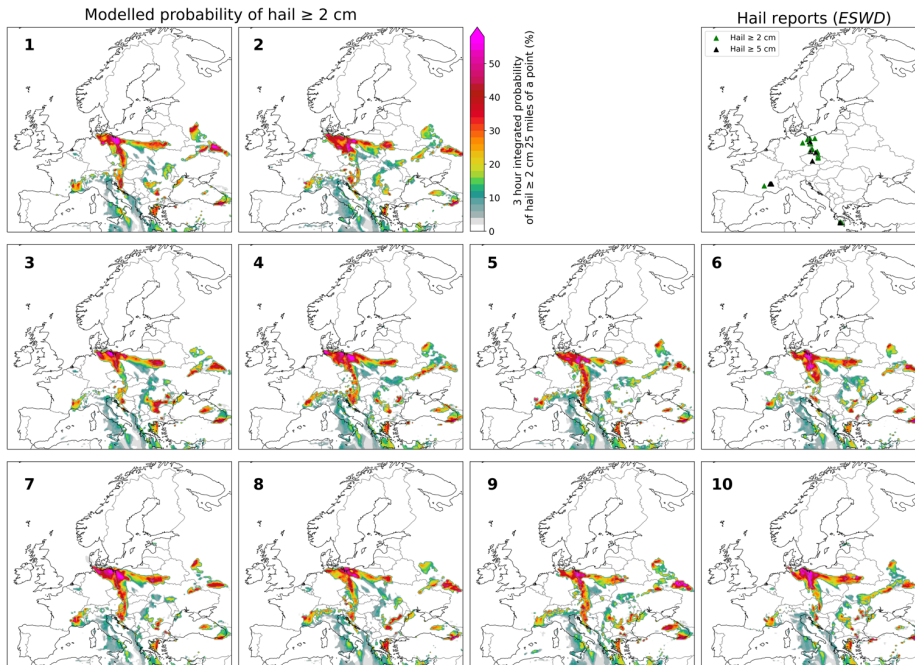
500 **Figure 3: Probabilistic ensemble forecast of hail occurrence based on a 1D logistic SHP model for the 15th of June 2019 at 12:00 UTC (initialized on the 15th of June 2019 at 00:00 UTC). Hail reports between 12:00 UTC and 15:00 UTC are shown as triangles (green for hail ≥ 2 cm but ≤ 5 cm, black for hail ≥ 5 cm) in the right-top panel.**
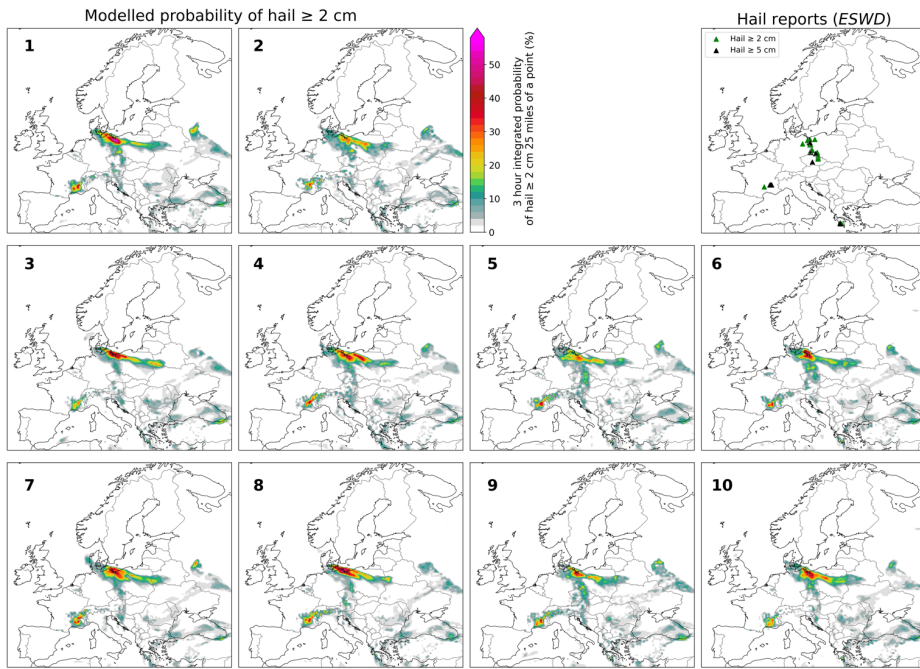
Figure 4: Probabilistic ensemble forecast of hail occurrence based on a 1D logistic CAPESHEAR model for the 15th of June 2019 at 12:00 UTC (initialized on the 15th of June 2019 at 00:00 UTC). Hail reports between 12:00 UTC and 15:00 UTC are respectively as triangles (green for hail ≥ 2 cm but ≤ 5 cm, black for hail ≥ 5 cm) in the right-top panel.

505

510

515
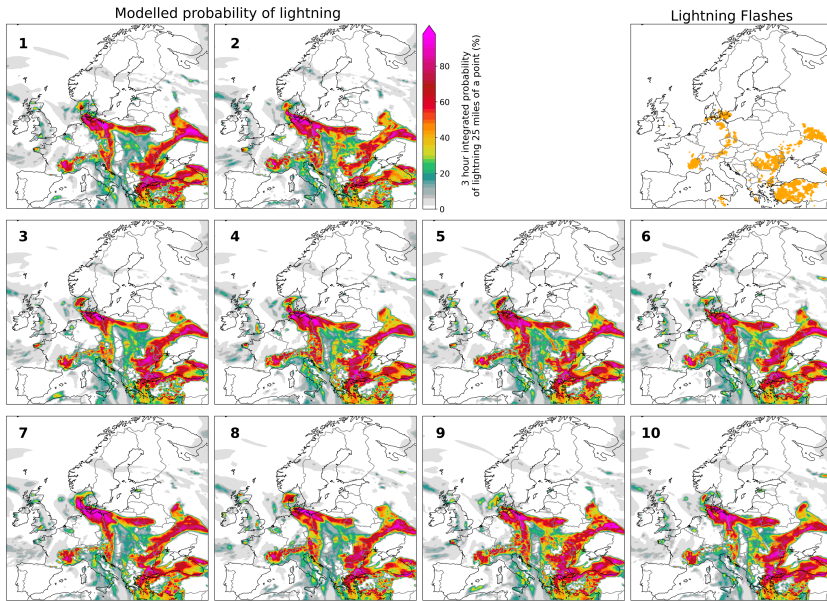
Figure 5: Probabilistic forecast of lightning occurrence on the 15th of June 2019 at 12:00 UTC (initialized on the 15th of June 2019 at 00:00 UTC) for the individual ensemble members. Lightning observations between 12:00 UTC and 15:00 UTC are shown as orange dots in the top-right panel.
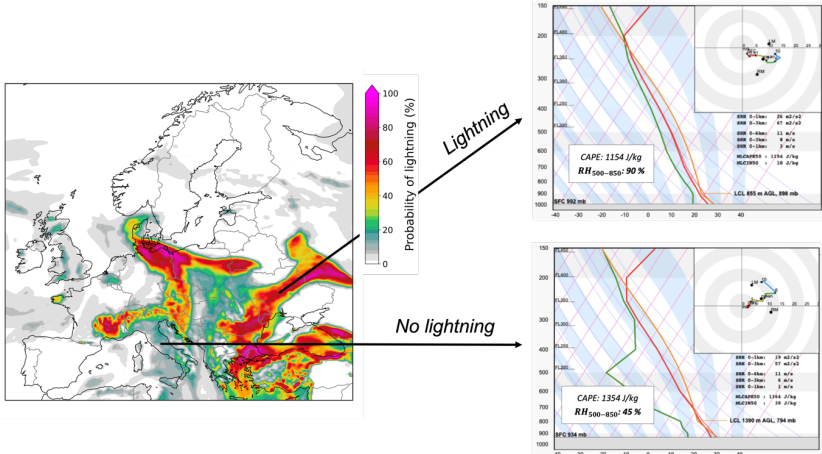
Figure 6: Ensemble mean probabilistic forecast of lightning occurrence on the 15th of June 2019 at 12:00 UTC (initialized on the 15th of June 2019 at 00:00 UTC). Forecast soundings from the ECMWF deterministic run are shown for two locations: Central Ukraine, and Central Italy. Corresponding CAPE and relative humidity between 500 and 850 hPa ($RH_{500-850}$) values are also shown. Hodographs are plotted in red (0-1 km), yellow (1-3 km), green (3-6 km) and blue (6-10 km) colour for the respective height intervals.
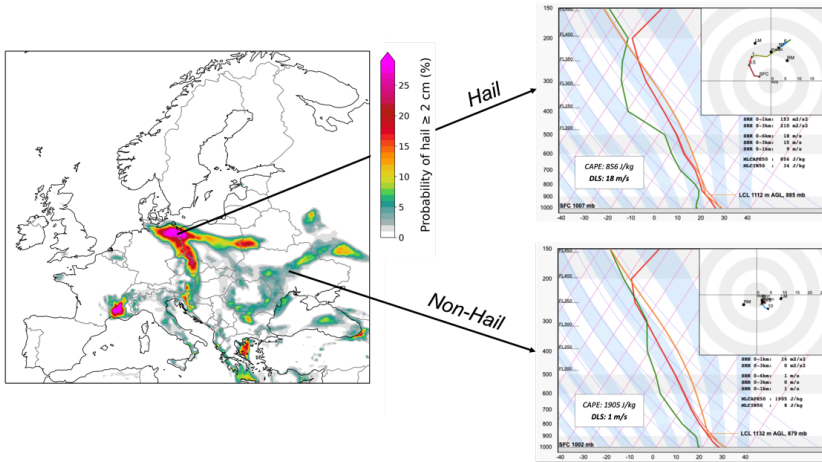
Figure 7: Ensemble mean probabilistic forecast of hail ≥ 2 cm occurrence on the 15th of June 2019 at 12:00 UTC (initialized on the 15th of June 2019 at 00:00 UTC). Forecast sounding from the ECMWF deterministic run are shown for two locations, eastern

 Germany, and Central Ukraine. Corresponding CAPE and deep layer shear are also shown. Hodographs are plotted in red (0-1 km), yellow (1-3 km), green (3-6 km) and blue (6-10 km) colour for the respective height intervals.
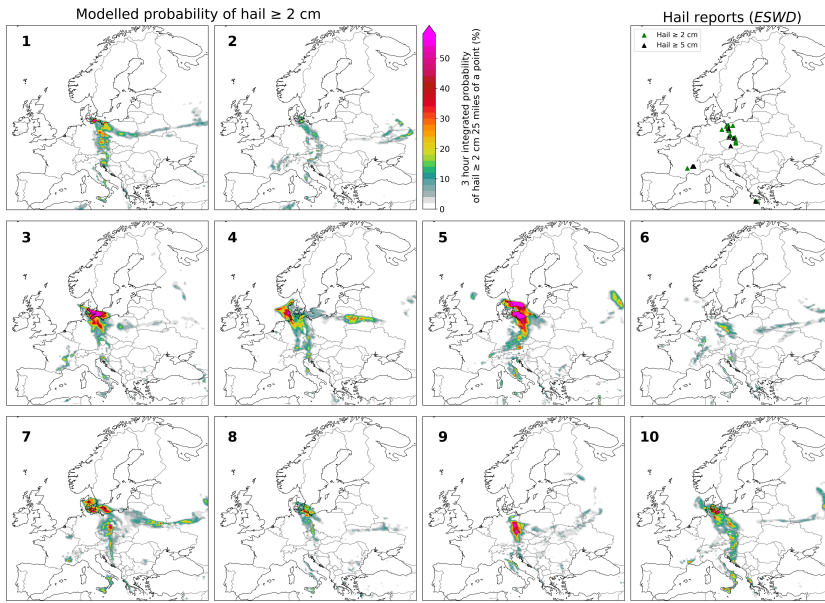
Figure 8: As in Figure 2 but for a forecast initialized on the 11th of June 2019 at 00:00 UTC.
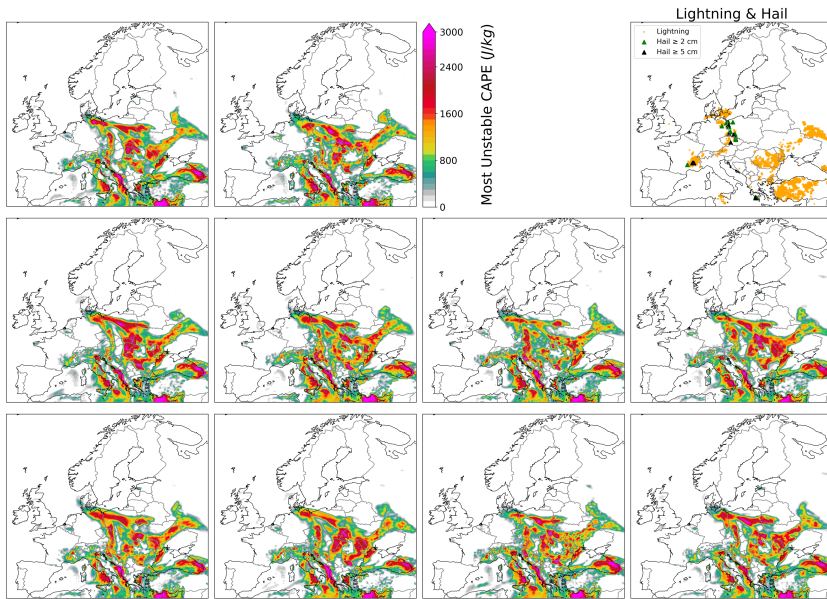
Figure 9: Forecast of MUCAPE for the 15th of June 2019 at 12:00 UTC, initialized at 00:00 UTC on the same day depending on the individual ensemble members. Lightning and hail reports between 12:00 UTC and 15:00 UTC are also shown respectively as yellow dots and triangles (green for hail ≥ 2 cm, black for hail ≥ 5 cm).
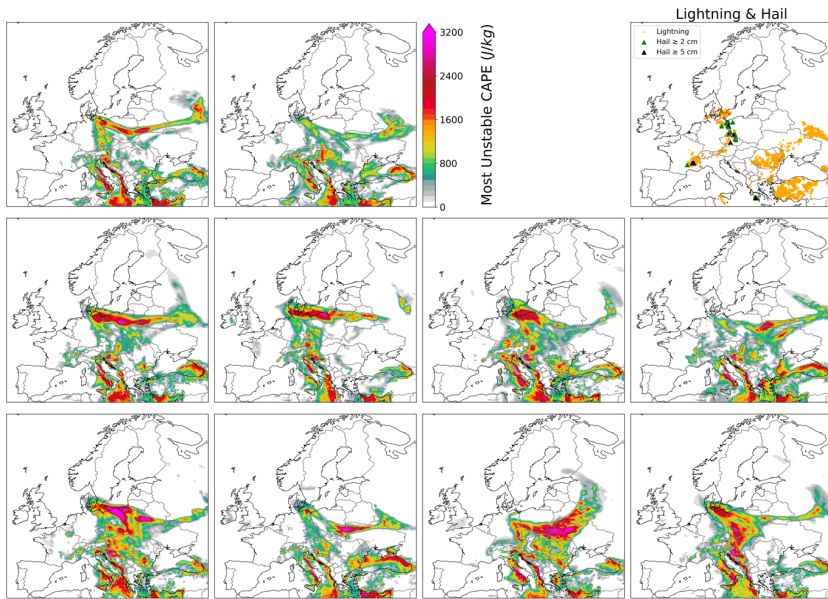
Figure 10: As in Fig. 9 for a forecast initialized on the 11ᵗʰ of June 2019 at 00:00 UTC.
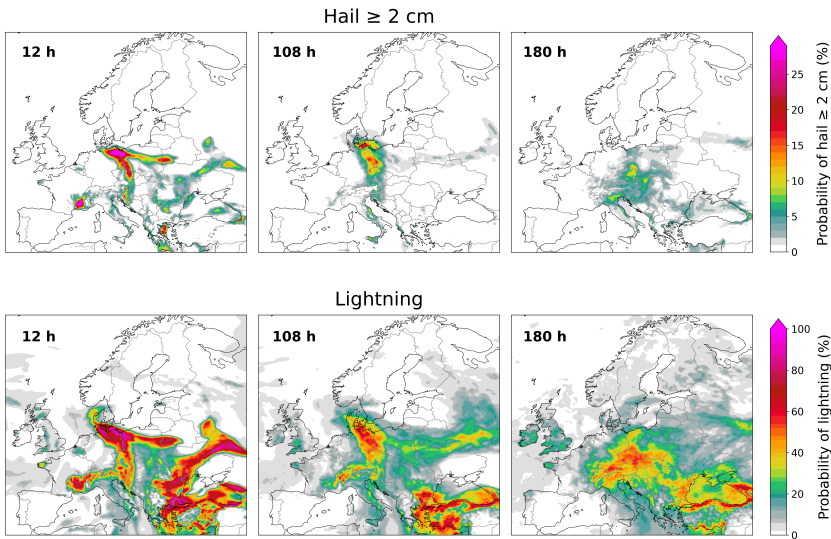
Hail ≥ 2 cm

Lightning

560

Figure 11: Ensemble mean probabilistic forecast of lightning and hail ≥ 2 cm occurrence for three different lead times (T-12h, T-108h and T-180h).

Deleted: 8
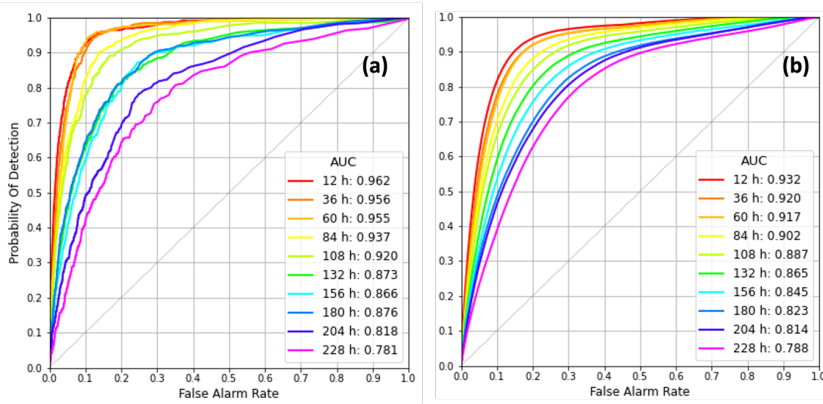
Figure 12: Receiver Operating Characteristic (ROC) curve for (a) the hail ≥ 2 cm and (b) the lightning model for lead times from 565 12 to 228 hours. Corresponding values of the Area Under the ROC Curve (AUC) are also shown.
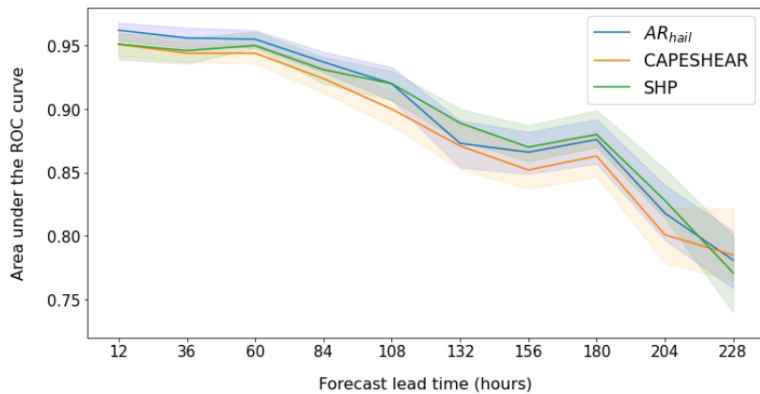
Deleted: 9

Figure 13: AUC depending on forecast lead time for AR_{hail}, CAPESHEAR and the Significant Hail Parameter. 1000-member block
570   bootstrap was performed to estimate 95% AUC confidence intervals for each model (shaded).

Appendices

**Appendix A - ECMWF forecast sounding for the 15th of June 2019 at 12:00 UTC (initialized at 00:00 UTC) across
Central Türkiye**
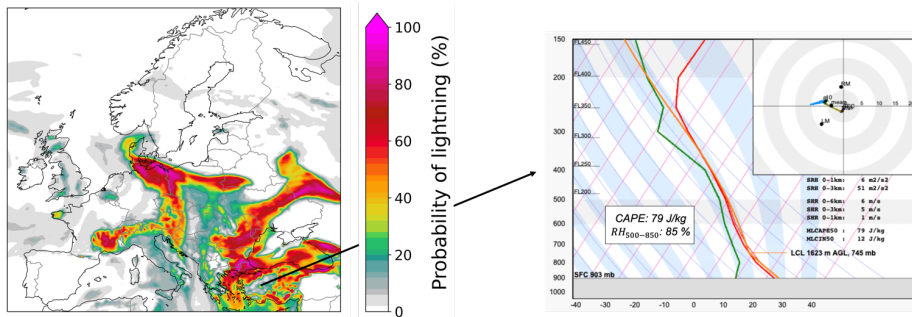
575

Figure A1: Ensemble mean probabilistic forecast of lightning occurrence on the 15th of June 2019 at 12:00 UTC (initialized at 00:00
UTC). The forecast sounding from the ECMWF deterministic run is shown for Central Türkiye. The corresponding CAPE and
relative humidity between 500 and 850 hPa ($RH_{500-850}$) are also shown.

Formatted: English (UK)

Formatted: Heading 3
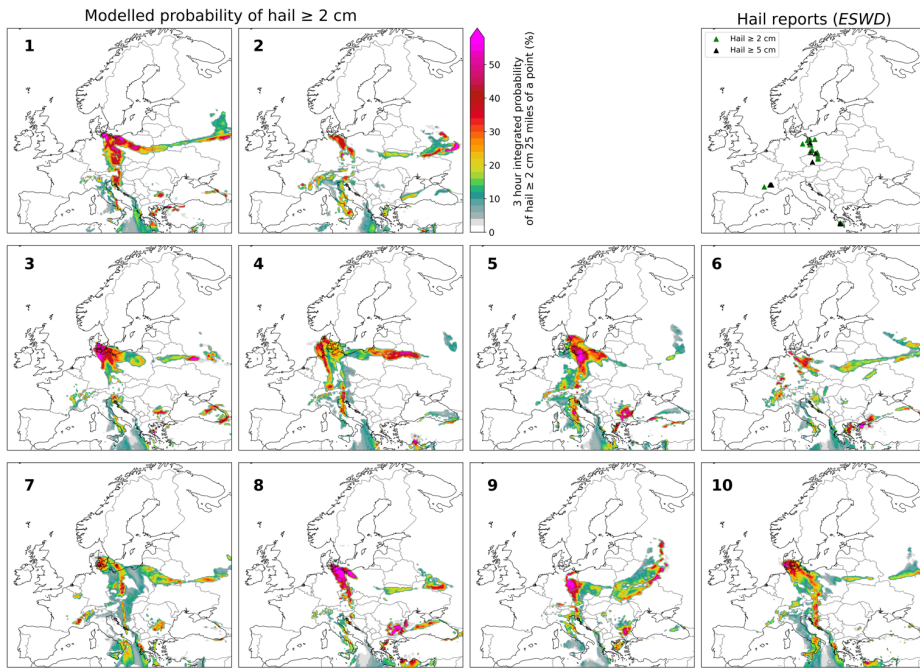
Figure B1: Probabilistic ensemble forecast of hail occurrence based on a 1D logistic SHP model for the 15th of June 2019 at 12:00 UTC (initialized on the 11th of June 2019 at 00:00 UTC). Hail reports between 12:00 UTC and 15:00 UTC are shown as triangles (green for hail ≥ 2 cm but ≤ 5 cm, black for hail ≥ 5 cm) in the right-top panel.

585
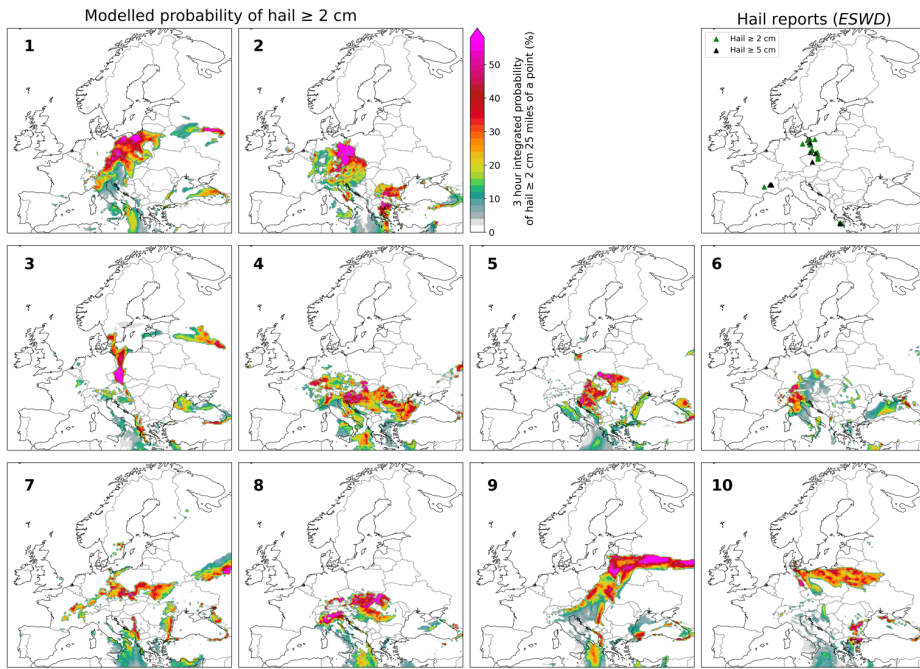
590   **Figure B2: As in B1 but for initialization on the 8th of June 2019 at 00:00 UTC.**
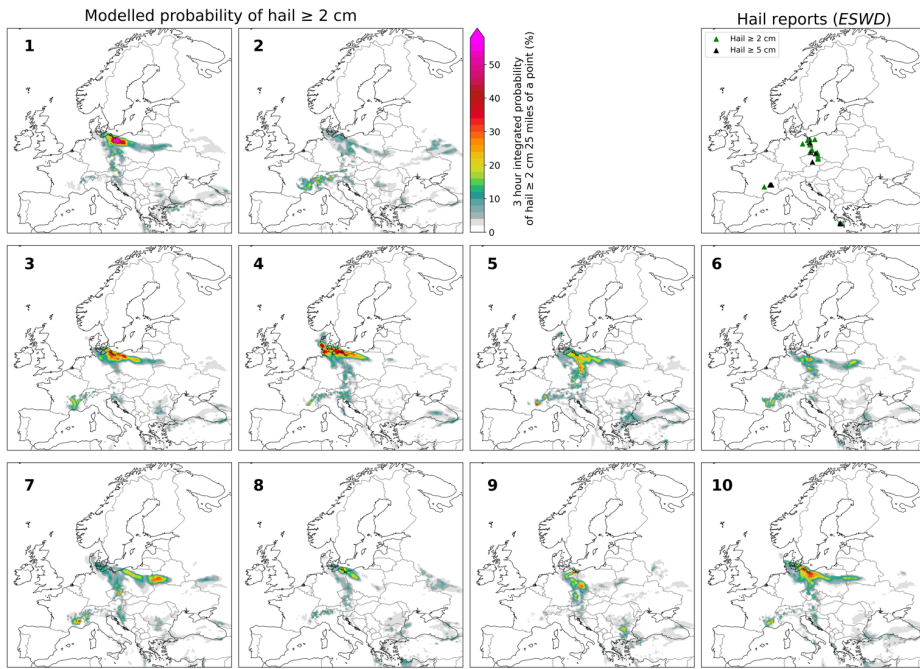
Figure B3: Probabilistic ensemble forecast of hail occurrence based on a 1D logistic CAPESHEAR model for the 15th of June 2019 at 12:00 UTC (initialized on the 11th of June 2019 at 00:00 UTC). Hail reports between 12:00 UTC and 15:00 UTC are shown respectively as triangles (green for hail ≥ 2 cm but ≤ 5 cm, black for hail ≥ 5 cm) in the right-top panel.

595
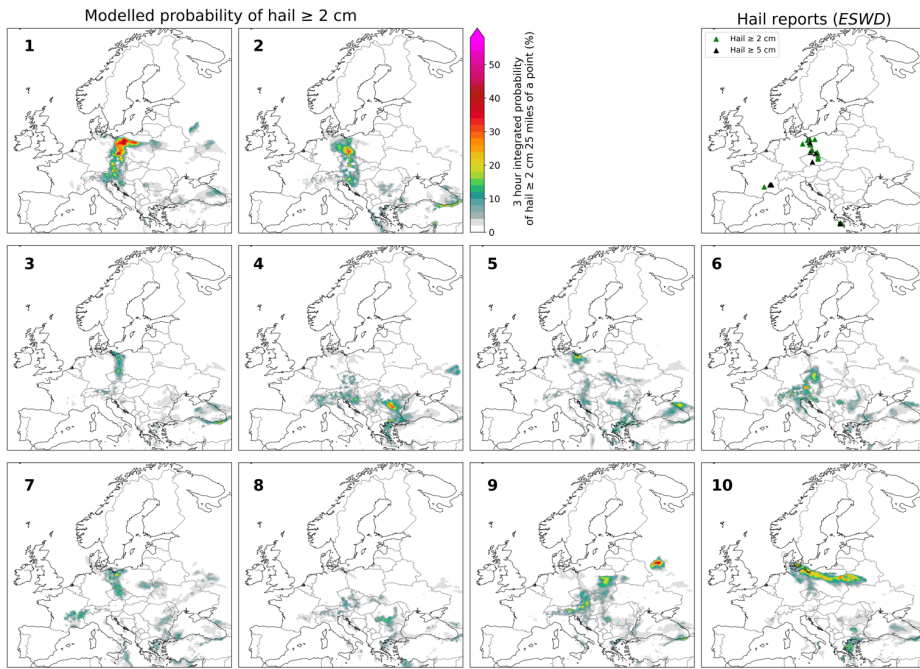
600

Appendix C - Additional lightning and hail forecasts for the 15th of June 2019 at 12:00 UTC

Modelled probability of hail ≥ 2 cm
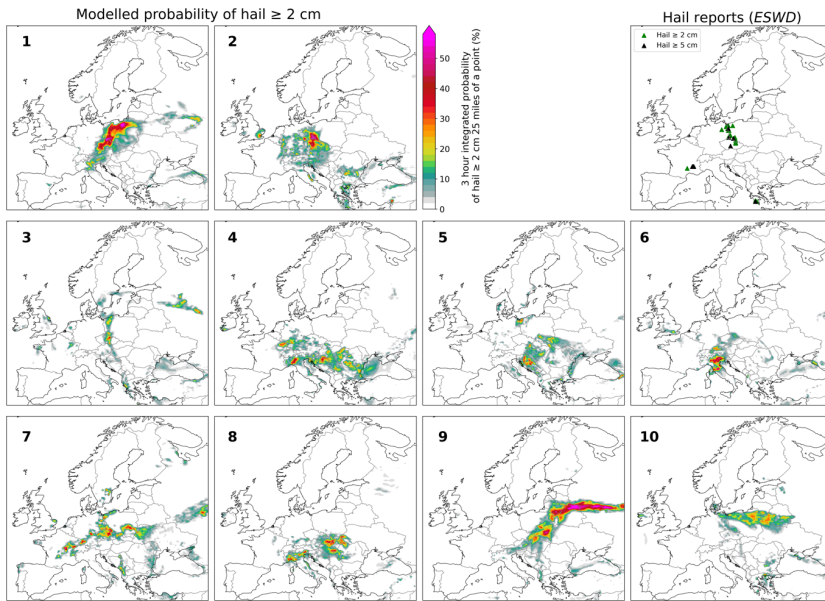
Hail reports (*ESWD*)

Figure C1: Probabilistic forecast of hail occurrence on the 15th of June 2019 at 12:00 UTC (initialized on the 8th of June 2019 at 00:00 UTC) for the different ensemble members. Hail reports between 12:00 UTC and 15:00 UTC are shown as triangles (green for hail ≥ 2 cm but ≤ 5 cm, black for hail ≥ 5 cm) in the right-top panel.

605
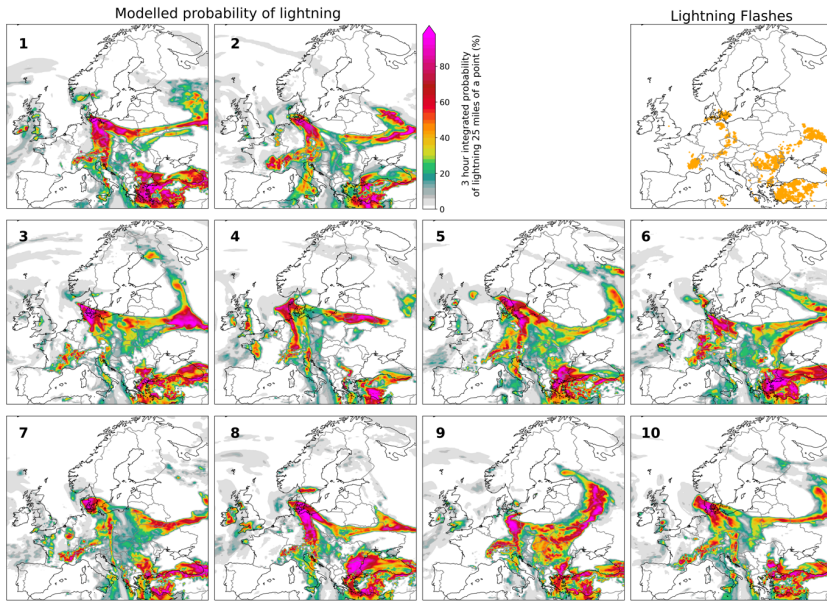
Figure C2: Probabilistic forecast of lightning occurrence on the 15th of June 2019 at 12:00 UTC (initialized on the 11th of June 2019 at 00:00 UTC) for the different ensemble members. Lightning observations between 12:00 UTC and 15:00 UTC are shown as yellow dots in the top-right panel.

Modelled probability of lightning

Lightning Flashes

Figure C3: As in C2 but for initialization on the 8th of June 2019 at 00:00 UTC.

620

625

Appendix D - Acronyms of model predictors

Short name	Long name
MU_LI	Most Unstable Lifted Index
RH_500–850hPa	Mean Relative Humidity between 500 and 850 hPa
1h Acc. Conv. Precip.	1 hour Accumulated Convective Precipitation
MU_MIXR	Most Unstable Mixing Ratio
MU500_CAPE-10°	Most Unstable CAPE (for a parcel originating above 500 m AGL) released above the -10°C isotherm
EFF_MU_BS	Effective Most Unstable Bulk Shear
MU_CAPE	Most Unstable CAPE
Deep Layer Shear	Bulk wind difference between 925 and 500 hPa

Table D1: Acronyms for parameters from ERA5 reanalysis used in AR-CHaMo.

Code availability

Code for computing the probabilistic forecasts is available from the corresponding author upon request (francesco.battaglioli@essl.org).

Data availability

Probabilistic forecasts are available from the corresponding author upon request (francesco.battaglioli@essl.org). Reforecast data are available through the ECMWF archive (https://www.ecmwf.int/en/forecasts/dataset/operational-archive).

Author contributions

FB developed the code to compute probabilistic lightning and hail forecasts with support from PG. FB analyzed data and produced all figures. IT extracted ECMWF reforecast data. FB wrote the manuscript with revising contributions from IT, PG and TP.

Competing interests

The contact author has declared that neither of the authors has any competing interests.

Acknowledgements

We would like to thank and acknowledge ECMWF for providing reforecast data, the Met Office for ATDnet lightning detection data and the many volunteers and ESSL staff for their reports to the ESWD. Dr. Mateusz Taszarek is acknowledged to have calculated and provided ERA5 predictors for the original AR-CHaMo models. Dr. Matthieu Chevallier is also acknowledged to have provided comments on the manuscript and have contributed to the review process.

Financial support

Battaglioli's contribution to the study was funded by the German Ministry of Education and Research for project 01LP1902G "CHECC", part of the Research Programme "ClimXtreme". Groenemeijer and Pŭčik's contributions were funded by the Austrian Science Fund (FWF) project P33113-N "PreCAST". Tsonevsky's contribution was funded by ECMWF.

References

Adams-Selin, R. and Ziegler, C. L.: Forecasting Hail Using a One-Dimensional Hail Growth Model within WRF, Mon. Weather Rev., 144(12), 4919-4939, https://doi.org/10.1175/MWR-D-16-0027.1, 2016.

Allen, J., Giammanco, I., Kumjian, M., Jurgen Punge, H., Zhang Q., Groenemeijer, P., Kunz, M., and Ortega, K.: Understanding Hail in the Earth System, Rev. Geophys., 58, https://doi.org/10.1029/2019RG000665, 2020.

Anderson, G. and Klugmann, D.: A European lightning density analysis using 5 years of ATDnet data, Nat. Hazard. Earth Sys., 14(4), 815-829, https://doi.org/10.5194/nhess-14-815-2014, 2014.

Bang, S., and Cecil, D.: Constructing a Multifrequency Passive Microwave Hail Retrieval and Climatology in the GPM Domain, J. Appl. Meteorol. Clim., 58, 1889-1904, https://doi.org/10.1175/JAMC-D-19-0042.1, 2019.

Battaglioli, F., Groenemeijer, P., Pŭčik, T., Taszarek, M., Ulbrich, U., and H. Rust, 2023: Modelled multidecadal trends of lightning and (very) large hail in Europe and North America (1950–2021) [Manuscript submitted for publication].

Bright, D.R., Wandishin, M.S., Jewell, R.E. and Weiss, S.J.: A physically based parameter for lightning prediction and its calibration in ensemble forecasts, Conf. on Meteor. Appl. of Lightning Data, Amer. Meteor. Soc., San Diego, CA (Vol. 3496, p. 30), 2005.

Brimelow, J. C., Reuter, G. W., and Poolman, E. R.: Modeling maximum hail size in Alberta thunderstorms, Wea. Forecast., 17(5), 1048–1062. doi:10.1175/1520-0434(2002)017<1048:mmhsia>2.0.co;2, 2002.

Brisson, E., Blahak, U., Lucas-Picher, P., Purr, C., and Ahrens, B.: Contrasting lightning projection using the lightning potential index adapted in a convection-permitting regional climate model. doi:10.21203/rs.3.rs-339754/v1, 2021.

Cecil, D., and Blankenship, C.: Toward a Global Climatology of Severe Hailstorms as Estimated by Satellite Passive Microwave Imagers, J. Climate, 25, 687-703, https://doi.org/10.1175/JCLI-D-11-00130.1, 2012.

Cintineo, J. L., Pavolonis, M. J., and Sieglaff, J. M.: Probsevere lightningcast: A deep-learning model for satellite-based Lightning nowcasting, Wea. Forecast., 37(7), 1239–1257. doi:10.1175/waf-d-22-0019.1, 2022.

Dafis, S., Fierro, A., Giannaros, T. M., Kotroni, V., Lagouvardos, K., and Mansell, E.: Performance evaluation of an explicit Lightning forecasting system, J. Geophys. Res.: Atmospheres, 123(10), 5130–5148. doi:10.1029/2017jd027930, 2018.

Dotzek, N., Groenemeijer, P., Feuerstein, B., and Holzer, A. M.: Overview of ESSL's severe convective storms research using the European Severe Weather Database ESWD, Atmos. Res., 93, 575–586, https://doi.org/10.1016/j.atmosres.2008.10.020, 2009.

Changnon, S. A., Chagnon, D., and Hilberg, S. D.: Hailstorms across the nation: An atlas about hail and its damages. Contract Rep. 2009-12, 95 pp, 2009.

Cintineo, J., Smith, T., Lakshmanan, V., Brooks, H., and Ortega, K.: An Objective High-Resolution Hail Climatology of the Contiguous United States, Weather Forecast., 27, 1235-1248, https://doi.org/10.1175/WAF-D-11-00151.1, 2012.

Czernecki, B., Taszarek, M., Marosz, M., and Polrolniczak, M.: Application of machine learning to large hail prediction - The importance of radar reflectivity, lightning occurrence and convective parameters derived from ERA5, Atmos. Res., 227, 249–262, https://doi.org/10.1016/j.atmosres.2019.05.010, 2019.

Enno, S., Sugier, J., Alber, R., and Seltzer, M.: Lightning flash density in Europe based on 10 years of ATDnet data, Atmos. Res., 235, 104769, https://doi.org/10.1016/j.atmosres.2019.104769, 2020.

Feudale, L., Manzato, A., and Micheletti, S.: A cloud-to-ground lightning climatology for North-eastern Italy, Advances in Science and Research, 10(1), 77–84. doi:10.5194/asr-10-77-2013, 2013.

Fluck, E., Kunz, M., Geissbuehler, P., and Ritz, S.: Radar-based assessment of hail frequency in Europe, Nat. Hazard. Earth Sys., 21, 683-701, https://doi.org/10.5194/nhess-21-683-2021, 2021.

Fuchs, B.R., and Coauthors: Environmental controls on storm intensity and charge structure in multiple regions of the continental United States, J. Geophys. Res.: Atmospheres, 120(13), 6575-6596, https://doi.org/10.1002/2015JD023271, 2015.

Gallo, B. T., Clark, A. J., and Dembek, S. R.: Forecasting tornadoes using convection-permitting ensembles, Weather Forecast., 31, 273–295, https://doi.org/10.1175/WAF-D-15-0134.1, 2016.

Gallo, B. T., Clark, A. J., Smith, B. T., Thompson, R. L., Jirak, I., and Dembek, S. R.: Blended probabilistic tornado forecasts: Combining climatological frequencies with NSSL–WRF ensemble forecasts, Weather Forecast., 33(2), 443–460, https://doi.org/10.1175/WAF-D-17-0132.1, 2018.

Geng, Y., and Coauthors: A deep learning framework for lightning forecasting with multi-source spatiotemporal data, Quart. J. Roy. Meteor. Soc., 147(741), 4048–4062. doi:10.1002/qj.4167, 2021

Gensini, V.A. and Tippett, M.K.: Global Ensemble Forecast System (GEFS) predictions of Days 1–15 U.S. tornado and hail frequencies, Geophys. Res. Lett., 46(5), 2922–2930, https://doi.org/10.1029/2018gl081724, 2019.

Groenemeijer, P., and Coauthors: Severe Convective Storms in Europe: Ten Years of Research and Education at the European Severe Storms Laboratory, B. Am. Meteorol. Soc., 98, 2641-2651, https://doi.org/10.1175/BAMS-D-16-0067.1, 2017.

Hamill, T.M., Hagedorn, R., and Whitaker, J.S.: Probabilistic forecast calibration using ECMWF and GFS ensemble reforecasts. part II: Precipitation, Mon. Weather Rev., 136, 2620–2632, https://doi.org/10.1175/2007mwr2411.1, 2008.

745 Hersbach, H., and Coauthors: The ERA5 global reanalysis, Q. J. Roy. Meteor. Soc., 146, 1999–2049, https://doi.org/10.1002/QJ.3802, 2020.

Hosmer, D. W., Lemeshow, S., and Sturdivant, R. X.: Applied Logistic Regression, 2nd Ed. Chapter 5, John Wiley and Sons, New York, NY, (2000), pp. 160-16, 2013.

Jewell, R., and Brimelow, J.: Evaluation of Alberta hail growth model using severe hail proximity soundings from the United
750 States, Wea. Forecast, 24(6), 1592–1609. doi:10.1175/2009waf2222230.1, 2009.

Johns, R.H. and Doswell III, C.A.: Severe local storms forecasting, Wea. Forecasting, 7(4), 588-612, https://doi.org/10.1175/1520-0434(1992)007<0588:SLSF>2.0.CO;2, 1992.

Johnson, A., and Sugden, K.: Evaluation of Sounding-Derived Thermodynamic and Wind-Related Parameters Associated with Large Hail Events, *E-Journal of Severe Storms Meteorology*, 9, 1-42, https://doi.org/10.55599/ejssm.v9i5.57, 2014.

755 Jewell, R., and Brimelow, J.: Evaluation of Alberta Hail Growth Model Using Severe Hail Proximity Soundings from the United States, Weather Forecast., 24, 1592-1609, https://doi.org/10.1175/2009WAF2222230.1, 2009.

Kühne, T., Antonescu, B., Groenemeijer, P., and Púčik, T.: Lightning fatalities in Europe (2001-2020), 11th European Conference on Severe Storms, Bucharest (RO), doi:10.5194/ecss2023-146, 2023.

Kumjian, M., Lombardo, K., and Loeffler, S.: The Evolution of Hail Production in Simulated Supercell Storms, J. Atmos.
760 Sci., 78, 3417-3440, https://doi.org/10.1175/JAS-D-21-0034.1, 2021.

Lagasio, M., Parodi, A., Procopio, R., Rachidi, F., and Fiori, E.: Lightning potential index performances in multimicrophysical cloud-resolving simulations of a back-building mesoscale convective system: The Genoa 2014 Event, J. Geophys. Res.: Atmospheres, 122(8), 4238–4257. doi:10.1002/2016jd026115, 2017.

Leinonen, J., Hamann, U., and Germann, U.: Seamless lightning nowcasting with recurrent-convolutional deep
765 learning, Artificial Intelligence for the Earth Systems, *1*(4). doi:10.1175/aies-d-22-0043.1, 2022.

Lepore, C., Tippett, M. K., and Allen, J. T.: ENSO-based probabilistic forecasts of March–May US tornado and hail activity, Geophys. Res. Lett., 44, 9093– 9101, https://doi.org/10.1002/2017GL074781, 2017.

Lepore, C., Tippett, M. K., and Allen, J. T.: CFSv2 monthly forecasts of tornado and hail activity. Weather Forecast 33, 1283– 1297, https://doi.org/10.1175/WAF-D-18-0054.1, 2018.

770 Loken, E. D., Clark, A. J., and Karstens, C. D.: Generating Probabilistic Next-Day Severe Weather Forecasts from Convection-Allowing Ensembles Using Random Forests, Weather Forecast., 35, 1605-1631, https://doi.org/10.1175/WAF-D-19-0258.1, 2020.

Lopez, P.: A Lightning Parameterization for the ECMWF Integrated Forecasting System, Mon. Wea. Rev., **144**, 3057–3075, https://doi.org/10.1175/MWR-D-16-0026.1, 2016.

775 Martius, O., Kunz, M., Nisi, L., and Hering, A.: Conference report 1st European Hail Workshop, Meteorol. Z., 24, 441–442, https://doi.org/10.1127/metz/2015/0667, 2015.

McCaul, E. W., Goodman, S. J., LaCasse, K. M., and Cecil, D. J.: Forecasting lightning threat using cloud-resolving model simulations. Wea. Forecast, 24(3), 709–729. doi:10.1175/2008waf2222152.1, 2009.

Mostajabi, A., Finney, D. L., Rubinstein, M., and Rachidi, F.: Nowcasting lightning occurrence from commonly available meteorological parameters using machine learning techniques, npj Climate and Atmospheric Science, 2(1). doi:10.1038/s41612-019-0098-0, 2019.

790   Murillo E., Homeyer, C., and Allen, J.: A 23-Year Severe Hail Climatology Using GridRad MESH Observations, Mon. Weather Rev., 149, 945-958, https://doi.org/10.1175/MWR-D-20-0178.1, 2021.

Nisi, L., Hering, A., Germann, U., Schroeer, K., Barras, H., Kunz, M., and Martius, O.: Hailstorms in the Alpine region: Diurnal cycle, 4D-characteristics, and the nowcasting potential of lightning properties, Q. J. Roy. Meteor. Soc., 146, 4170-4194, https://doi.org/10.1002/qj.3897, 2020.

795   Ortega, K. L., Krause, J. M., and Ryzhkov, A. V.: Polarimetric Radar Characteristics of Melting Hail. Part III: Validation of the Algorithm for Hail Size Discrimination, J. Appl. Meteorol. Clim., 55(4), 829-848, https://doi.org/10.1175/JAMC-D-15-0203.1, 2016.

Poręba, S., Taszarek, M., and Ustrnul, Z.: Diurnal and Seasonal Variability of ERA5 Convective Parameters in Relation to Lightning Flash Rates in Poland, Wea. Forecast, 37(8), 1447-1470, https://doi.org/10.1175/WAF-D-21-0099.1, 2022.

800   Púčik, T., Groenemeijer, P., Rýva, D., and Kolář, M.: Proximity Soundings of Severe and Nonsevere Thunderstorms in Central Europe, Mon. Weather Rev., 143(12), 4805-4821, https://doi.org/10.1175/MWR-D-15-0104.1, 2015.

Púčik, T., Castellano, C., Groenemeijer, P., Kühne, T., Rädler, A., Antonescu, B., and Faust, E.: Large Hail Incidence and Its Economic and Societal Impacts across Europe, Mon. Weather Rev., 147, 3901-3916, https://doi.org/10.1175/MWR-D-19-0204.1, 2019.

805   Rädler, A., Groenemeijer, P., Faust, E., and Sausen, R.: Detecting Severe Weather Trends Using an Additive Regressive Convective Hazard Model (AR-CHaMo), J. Appl. Meteorol. Clim., 57(3), 569-587, https://doi.org/10.1175/JAMC-D-17-0132.1, 2018.

Ryzhkov, A. V., Kumjian, M. R., Ganson, S. M., and Zhang, P.: Polarimetric Radar Characteristics of Melting Hail. Part II: Practical Implications, J. Appl. Meteorol. Clim., 52(12), 2871-2886, https://doi.org/10.1175/JAMC-D-13-074.1, 2013.

810   Schmidt, M.: Improvement of hail detection and nowcasting by synergistic combination of information from polarimetric radar, model predictions, and in-situ observations. Ph.D. dissertation, Universität Bonn, 150 pp, 2020.

Taszarek, M., and Coauthors: A climatology of thunderstorms across Europe from a synthesis of multiple data sources. J. Climate, 32(6), 1813–1837. doi:10.1175/jcli-d-18-0372.1, 2019.

Taszarek, M., Allen, J., Groenemeijer, P., Edwards, R., Brooks, H., Chmielewski, V., and Enno, S.: Severe Convective Storms across Europe and the United States. Part I: Climatology of Lightning, Large Hail, Severe Wind, and Tornadoes, J. Climate, 33, 10239-10261, https://doi.org/10.1175/JCLI-D-20-0345.1, 2020(a).

815

Taszarek, M., Allen, J., Púčik, T., Hoogewind, K., and Brooks, H.: Severe Convective Storms across Europe and the United States. Part II: ERA5 Environments Associated with Lightning, Large Hail, Severe Wind, and Tornadoes, J. Climate, 33(23), 10263-10286, https://doi.org/10.1175/JCLI-D-20-0346.1, 2020b.

Thompson, R. L., Edwards R., and Mead C. M.: An update to the supercell composite and significant tornado parameters, 22nd Conf. Severe Local Storms, Hyannis, MA, Amer. Meteor. Soc., P8.1., https://ams.confex.com/ams/11aram22sls/techprogram/paper_82100.htm, 2004.

Thompson, R. L., Smith, B. T., Grams, J. S., Dean, A. R., and Broyles, C.: Convective modes for significant severe thunderstorms in the contiguous United States. Part II: Supercell and QLCS tornado environments, Wea. Forecast., 27, 1136–1154, https://doi.org/10.1175/WAF-D-11-00116.1, 2012.

Tsonevsky, I., Doswell, C.A., and Brooks, H.E.: Early warnings of severe convection using the ECMWF Extreme Forecast Index, Wea. Forecast., 33, 857–871, https://doi.org/10.1175/waf-d-18-0030.1, 2018.

Uhlířová, I., Popová, J., and Sokol, Z.: Lightning potential index and its spatial and temporal characteristics in Cosmo NWP model, Atmos. Res., 268, doi:10.1016/j.atmosres.2022.106025, 2022.

Van Den Broeke, M.S., Schultz, D.M., Johns, R.H., Evans, J.S. and Hales, J.E.: Cloud-to-ground lightning production in strongly forced, low-instability convective lines associated with damaging wind, Wea. Forecast., 20(4), 517-530, https://doi.org/10.1175/WAF876.1, 2005.

Vitart, F.: Evolution of ECMWF sub-seasonal forecast skill scores, Q. J. Roy. Meteor. Soc., 140, 1889–1899, https://doi.org/10.1002/qj.2256, 2013.

Wapler, K.: High-resolution climatology of lightning characteristics within Central Europe, Meteorology and Atmospheric Physics, 122(3–4), 175–184. doi:10.1007/s00703-013-0285-1, 2013.

Warren, R.A., Ramsay, H.A., Siems, S.T., Manton, M.J., Peter, J.R., Protat, A., and Pillalamarri, A.: Radar-based climatology of damaging hailstorms in Brisbane and Sydney, Australia, Q. J. Roy. Meteor. Soc., 146, 505–530, https://doi.org/10.1002/qj.3693, 2020.

Westermayer, A., Groenemeijer, P., Pistotnik, G., Sausen, R. and Faust, E.: Identification of favorable environments for thunderstorms in reanalysis data, Meteorologische Zeitschrift, 26(1), 59-70, 10.1127/metz/2016/0754, 2017.

Yair, Y., and Coauthors: Predicting the potential for lightning activity in Mediterranean storms based on the weather research and forecasting (WRF) model dynamic and Microphysical Fields, J. Geophys. Res., 115(D4). doi:10.1029/2008jd010868, 2010.

Zepka, G. S., Pinto, O., and Saraiva, A. C. V.: Lightning forecasting in southeastern Brazil using the WRF model, Atmos. Res., 135–136, 344–362. doi:10.1016/j.atmosres.2013.01.008, 2014.

Page 2: [1] Deleted	**Francesco Battaglioli**	**31/07/2023 12:03:00**

Page 2: [2] Deleted	**Francesco Battaglioli**	**31/07/2023 12:03:00**

Page 2: [3] Deleted	**Francesco Battaglioli**	**31/07/2023 14:31:00**

Page 2: [4] Deleted	**Francesco Battaglioli**	**31/07/2023 14:24:00**
Page 2: [5] Deleted	**Tomas Pucik**	**27/07/2023 16:10:00**

Page 2: [6] Deleted	**Francesco Battaglioli**	**31/07/2023 15:00:00**

Page 27: [7] Deleted	**Francesco Battaglioli**	**31/07/2023 17:31:00**
Page 30: [8] Deleted	**Francesco Battaglioli**	**31/07/2023 09:23:00**
Page 31: [9] Formatted	**Francesco Battaglioli**	**01/08/2023 16:28:00**

English (US)

Page 31: [9] Formatted	**Francesco Battaglioli**	**01/08/2023 16:28:00**

English (US)

Page 31: [9] Formatted	**Francesco Battaglioli**	**01/08/2023 16:28:00**

English (US)

Page 31: [9] Formatted	**Francesco Battaglioli**	**01/08/2023 16:28:00**

English (US)

Page 31: [9] Formatted	**Francesco Battaglioli**	**01/08/2023 16:28:00**

English (US)

Page 31: [10] Formatted	**Francesco Battaglioli**	**01/08/2023 12:20:00**

English (US)

Page 31: [10] Formatted	**Francesco Battaglioli**	**01/08/2023 12:20:00**

English (US)

Page 31: [10] Formatted	**Francesco Battaglioli**	**01/08/2023 12:20:00**

English (US)

Page 31: [10] Formatted	**Francesco Battaglioli**	**01/08/2023 12:20:00**

English (US)

Page 31: [10] Formatted	**Francesco Battaglioli**	**01/08/2023 12:20:00**

English (US)

English (US)

Font: Not Italic

Font: Not Italic

English (US)

English (US)

English (US)

English (US)

English (US)

English (US)

English (US)

English (US)

English (US)

English (US)

English (US)

English (US)

English (US)

English (US)

English (US)

English (US)

English (US)

English (US)

English (US)

English (US)

English (US)

English (US)

English (US)

English (US)

English (US)

English (US)

English (US)

English (US)

English (US)

English (US)

English (US)

English (US)

Font: Not Italic

Font: Not Italic, English (US)

Font: Not Italic

Font: Not Italic, English (US)

Font: Not Italic

English (US)

Font: Not Italic

Font: Not Italic

English (US)

English (US)

Font: Not Italic

Font: Not Italic

Font: Not Italic

Page 33: [34] Formatted   Francesco Battaglioli   01/08/2023 11:15:00

English (US)

Page 33: [35] Formatted   Francesco Battaglioli   01/08/2023 11:15:00

English (US)

Page 33: [36] Formatted   Francesco Battaglioli   01/08/2023 11:41:00

Font: Not Italic

Page 33: [37] Formatted   Francesco Battaglioli   01/08/2023 11:41:00

Font: Not Italic, English (US)

Page 33: [38] Formatted   Francesco Battaglioli   01/08/2023 11:41:00

Font: Not Italic

Page 33: [39] Formatted   Francesco Battaglioli   01/08/2023 11:41:00

Font: Not Italic, English (US)

Page 33: [40] Formatted   Francesco Battaglioli   01/08/2023 11:41:00

Font: Not Italic

Page 33: [41] Formatted   Francesco Battaglioli   01/08/2023 11:41:00

Font: Not Italic, English (US)

Page 33: [42] Formatted   Francesco Battaglioli   01/08/2023 11:41:00

Font: Not Italic

Page 33: [43] Formatted   Francesco Battaglioli   01/08/2023 11:15:00

English (US)

Page 33: [44] Formatted   Francesco Battaglioli   01/08/2023 11:53:00

English (US)

Page 33: [45] Formatted   Francesco Battaglioli   01/08/2023 11:53:00

English (US)

Page 33: [46] Formatted   Francesco Battaglioli   01/08/2023 11:53:00

English (US)

Page 33: [47] Formatted   Francesco Battaglioli   01/08/2023 11:53:00

Font: Not Italic

Page 33: [48] Formatted   Francesco Battaglioli   01/08/2023 11:53:00

English (US)

English (US)